

Edge states and topological orders in the spin liquid phases of star lattice

Guang-Yao Huang, Shi-Dong Liang,* and Dao-Xin Yao†

State Key Laboratory of Optoelectronic Material and Technology,

Guangdong Province Key Laboratory of Display Material and Technology,

School of Physics and Engineering, Sun Yat-sen University, Guangzhou, 510275, People's Republic of China

A group of novel materials can be mapped to the star lattice, which exhibits some novel physical properties. We give the bulk-edge correspondence theory of the star lattice and study the edge states and their topological orders in different spin liquid phases. The bulk and edge-state energy structures and Chern number depend on the spin liquid phases and hopping parameters because the local spontaneous magnetic flux in the spin liquid phase breaks the time reversal and space inversion symmetries. We give the characteristics of bulk and edge energy structures and their corresponding Chern numbers in the uniform, nematic and chiral spin liquids. In particular, we obtain analytically the phase diagram of the topological orders for the chiral spin liquid states $SL[\phi, \phi, -2\phi]$, where ϕ is the magnetic flux in two triangles and a dodecagon in the unit cell. Moreover, we find the topological invariance for the spin liquid phases, $SL[\phi_1, \phi_2, -(\phi_1 + \phi_2)]$ and $SL[\phi_2, \phi_1, -(\phi_1 + \phi_2)]$. The results reveal the relationship between the energy-band and edge-state structures and their topological orders of the star lattice.

I. INTRODUCTION

The discovery of the Integer Quantum Hall effect (IQHE) stimulates novel fundamental concepts in condensed matter physics, such as the gauge invariance,¹ edge state,² and Chern number³. In particular, Y. Hatsugai reveals the relationship between Chern number and edge states in the IQHE,^{4,5} which provides another way from the edge state to understand the topological order in finite systems.⁶ Moreover, the successful synthesis of nano and novel materials, such as the triangular organic material $\kappa - BEDT(CN)_3$,⁷ the kagome lattice herbertsmithite⁸ and the three-dimensional hyperkagome lattice magnet $(Na_4Ir_3O_8)$,⁹ provide many opportunities to examine theoretically and experimentally some novel physical properties, including the topological properties,^{4,5} fractionalized excitation^{10,11}, singlet valence-bond solid states,¹²⁻¹⁴ and edge states. Theoretically, these materials can be mapped to novel geometric lattices, such as the star lattice which is also called the triangle-honeycomb lattice^{15,16}, Fisher lattice or decorated honeycomb lattice.¹⁷ These geometric lattice models provide a new view to understand the geometric effect and spin frustration.^{6,18,19} In particular, the spin models on the star and honeycomb lattices have shown many novel phases including the Abelian and non-Abelian anyons, chiral spin-liquid phases, topological orders,¹⁵⁻¹⁷ magnetic orders^{19,20}, and topological insulator.^{21,22}

The IQHE reveals some novel transport properties of electrons in two-dimensional (2D) systems, in which the edge states play a key role and the Hall conductance can be expressed in terms of Chern number.^{2,3} Interestingly, the bulk-edge correspondence discovered by Y. Hatsugai^{4,5} becomes an efficient method to explore the edge states in various 2D systems, such as the honeycomb lattice (Graphene)²³ and spin-chiral ferromagnetic kagome lattice.^{6,24} However, the star lattice consists of a special lattice geometry, which can be mapped to a class

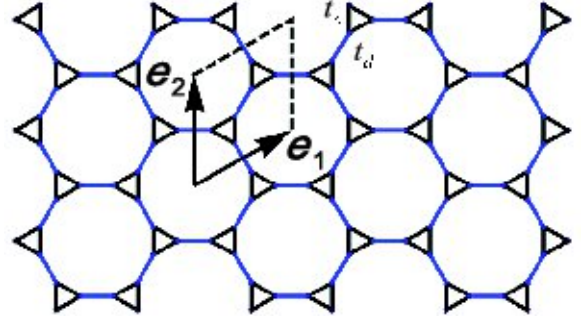


FIG. 1: (Color online) A star lattice with basis e_1 and e_2 . There are six sites in the unit cell. t_c represents the hopping amplitude inside the triangle (the bond in black), and t_d corresponds to the hopping amplitude between different triangles (the bond in blue).

of materials and cold atoms in optical lattices. The mean field study of Heisenberg model demonstrates the existence of several spin liquid phases, which depend on the flux configurations of two triangles and one dodecagon in the unit cell.¹⁹ A natural question arises: what is the relationship between the spin liquid phases and edge states on the star lattice with boundaries?

In this paper, we focus on the edge states and their topological orders on the star lattice with boundaries. We begin with a 2D tight-binding model with the Hund's rule coupling. It can be mapped to an effective tight-binding spinless model.¹⁸ The mean field approach predicts that there exists several spin liquid phases in the ground states with the local time reversal symmetry breaking.¹⁹ We use the bulk-edge correspondence method to analyze the edge states and their topological orders on the star lattice with boundaries.

This paper is organized as follows. In Sec. II, we introduce the tight-binding model with boundaries and map it to a spinless tight-binding model. In Sec. III, we give the bulk-edge correspondence for the star lattice. We

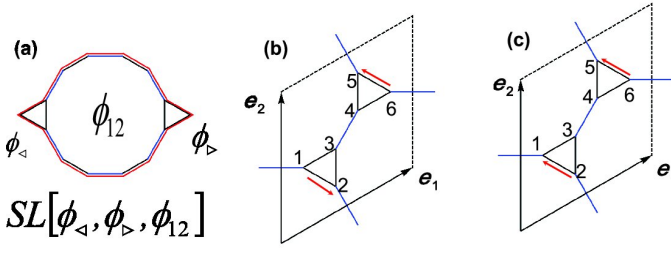


FIG. 2: (Color online) The elementary plaquette of star lattice contains two inequivalent triangles \triangleleft , \triangle , and one dodecagon. The magnetic flux configurations are labeled by $SL[\phi_{\triangleleft}, \phi_{\triangle}, \phi_{12}]$ following Ref.¹⁹.

present the edge states and their corresponding Chern numbers in various phases in Sec. IV. Finally, we give the discussion and conclusions.

II. MODEL AND SPIN LIQUID PHASES

In order to understand the relationship between the lattice geometry, edge states, and their topological properties, we consider the star lattice with boundaries, in which the conducting electrons move in a local spin background and couple with them by the Hund's rule to form a double-exchange system. The corresponding tight-binding Hamiltonian can be written as,

$$H = \sum_{\langle i,j \rangle \sigma} t_{ij} (c_{j\sigma}^\dagger c_{i\sigma} + H.c.) - J \sum_i c_{i\alpha}^\dagger \sigma_{\alpha\beta} \cdot \mathbf{S}_i c_{i\beta} \quad (1)$$

where t_{ij} is the hopping amplitude between two nearest neighboring sites $\langle i, j \rangle$; $c_{i\sigma}^\dagger$ ($c_{i\sigma}$) is the creation (annihilation) operator on site i with spin σ ; \mathbf{S}_i is the local spin on site i , which couples with the conducting electron spins with the effective coupling constant J . We consider that the local spins are approximately classical and the coupling J is strong enough to have the hopping electrons to align them to the local spin \mathbf{S}_i on each site with the spinon function, $|\chi\rangle = (e^{a_i} \cos(\theta_i/2), e^{i(a_i + \phi_i)} \sin(\theta_i/2))$, where (θ_i, ϕ_i) are the spinon parameters. In this spinon representation, the Hamiltonian Eq.(1) can be mapped to an effective tight-binding Hamiltonian,

$$H_{eff} = \sum_{\langle i,j \rangle} (t_{ij}^{eff} c_j^\dagger c_i + H.c.) \quad (2)$$

where the effective hopping amplitude¹⁸

$$\begin{aligned} t_{ij}^{eff} &= t_{ij} \left[\cos\left(\frac{\theta_i}{2}\right) \cos\left(\frac{\theta_j}{2}\right) + e^{-(\phi_i - \phi_j)} \sin\left(\frac{\theta_i}{2}\right) \sin\left(\frac{\theta_j}{2}\right) \right] e^{ia_{ij}} \\ &= t(\theta_{ij}, \phi_{ij}) e^{ia_{ij}} \end{aligned}$$

where the phase a_{ij} is the vector potential generated by spin and corresponds to the Berry phase felt by the hopping electron. It is noted that the unit cell of the star lattice contains two triangular plaquettes and one 12-site

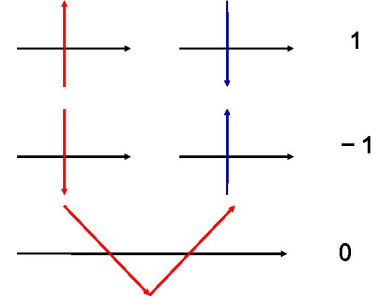


FIG. 3: (Color online) The intersection number between the canonical loop on the complex-energy surface (Riemann surface) and the trace of the edge state energy Ref.⁵.

dodecagon plaquette. The mean field study of Heisenberg model on the star lattice has revealed the existence of several spin liquid phases.¹⁹ The spin liquid phases depend on the flux figuration of the unit cell, which is labeled by the notation $SL[\phi_{\triangleleft}, \phi_{\triangle}, \phi_{12}]$.¹⁹ In terms of the original spin variable, the fluxes on the triangular plaquettes correspond to the scalar spin chiralities $\mathbf{S}_1 \cdot \mathbf{S}_2 \times \mathbf{S}_3$, while ϕ_{12} is related to the 12 spins around the dodecagon loop. In the uniform spin liquid phase, $SL[0, 0, 0]$, $t_{ij}^{eff} = t(\theta_{ij}, \phi_{ij}) \in \mathbb{R}$. For the non-uniform spin liquid state, the spin chirality arises, the fermion hopping will acquire a phase $t_{ij}^{eff} = t(\theta_{ij}, \phi_{ij}) e^{ia_{ij}}$, rendering a nonzero flux for a fermion moving around a loop $\phi = \sum_{loop} a_{ij}$. $t(\theta_{ij}, \phi_{ij})$, in principle, depends on the angles between spins \mathbf{S}_i and \mathbf{S}_j . However in the mean field approximation, $t(\theta_{ij}, \phi_{ij})$ should be independent on the angles, (θ_{ij}, ϕ_{ij}) for the spin liquid phases because the fluxes through plaquettes are periodic in the whole lattice.¹⁹ Thus the hopping parameters t_{ij}^{eff} can be classified into two independent variables on the star lattice. t_c labels the hopping amplitude inside the triangles and t_d is the hopping amplitude between different triangles. For convenience, we introduce $r \equiv \frac{t_d}{t_c}$ to measure the ratio of these two hopping amplitudes.

For a given flux configuration, $\phi = \sum_{loop} a_{ij}$, there are different phase configurations a_{ij} . The effect of the phase configuration can shift the whole energy band in (3) the k space, but do not modify the energy band structure. Namely, different choices of the phase configurations do not change the edge state and their topological properties of the star lattice. This allows us to set a simple choice of the phase configuration for various spin liquid phases to study their edge states and topological orders.

III. EDGE STATES AND TOPOLOGICAL ORDERS

A. Bulk-edge correspondence theory of star lattice

In general, we consider a strip of star lattice with the boundary along the \mathbf{e}_1 direction and the periodic infinite \mathbf{e}_2 direction shown in Fig.1. We assume that the spin liquid phase $SL[\phi_{\triangleleft}, \phi_{\triangleright}, \phi_{12}]$, where the fluxes satisfy the constraint, $\phi_{\triangleleft} + \phi_{\triangleright} + \phi_{12} = 0$. Using the Bloch theorem in the \mathbf{e}_2 direction, $c_j = \frac{1}{L_2} \sum_{\mathbf{k}} e^{i\mathbf{k} \cdot \mathbf{e}_2} c_{n\ell}(k)$, where n labels the unit cell and ℓ labels the sites in the unit cell. We set $\mathbf{k} \cdot \mathbf{e}_2 = k$ for convenience. The Hamiltonian in Eq.(2) can be written as

$$H_{eff} = \sum_{\mathbf{k}} \mathbf{C}^\dagger(\mathbf{k}) \mathbf{h}(\mathbf{k}) \mathbf{C}(\mathbf{k}), \quad (4)$$

where $\mathbf{C}^\dagger(k) = (c_{1,1}^\dagger(k) \dots c_{1,6}^\dagger(k) c_{2,1}^\dagger(k) \dots c_{2,6}^\dagger(k) \dots c_{N_1,6}^\dagger(k))$, and

$$\mathbf{h}(k) = \begin{bmatrix} d(k) & v & 0 & \dots & 0 \\ v^\top & d(k) & v & 0 & \vdots \\ 0 & v^\top & \ddots & v & 0 \\ \vdots & 0 & v^\top & d(k) & v \\ 0 & \dots & 0 & v^\top & d(k) \end{bmatrix}_{N_1 \times N_1} \quad (5)$$

with

$$d(k) = t_c \begin{bmatrix} 0 & e^{-i\phi_1} & 1 & 0 & 0 & 0 \\ e^{i\phi_1} & 0 & 1 & 0 & r e^{-ik} & 0 \\ 1 & 1 & 0 & r & 0 & 0 \\ 0 & 0 & r & 0 & 1 & 1 \\ 0 & r e^{-ik} & 0 & 1 & 0 & e^{i\phi_2} \\ 0 & 0 & 0 & 1 & e^{-i\phi_2} & 0 \end{bmatrix} \quad (6)$$

$$v = \begin{bmatrix} 0 & 0 & 0 & 0 & 0 & 0 \\ 0 & 0 & 0 & 0 & 0 & 0 \\ 0 & 0 & 0 & 0 & 0 & 0 \\ 0 & 0 & 0 & 0 & 0 & 0 \\ 0 & 0 & 0 & 0 & 0 & 0 \\ r & 0 & 0 & 0 & 0 & 0 \end{bmatrix}, \quad (7)$$

where N_1 is the number of unit cell along the \mathbf{e}_1 direction. The Bloch wave function can be written as $|\Psi(k)\rangle = \sum_{n,\ell} \psi_{n,\ell} c_{n,\ell}(k) |0\rangle$, where n runs the unit cell in the \mathbf{e}_1 direction. Inserting it into the Schrödinger equation, $H|\Psi\rangle = E|\Psi\rangle$, the solution can be reduced to a set of equations (Harper equation)

$$\begin{cases} \psi_{n,2} e^{-i\phi_1} + \psi_{n,3} + r \psi_{n-1,6} = \varepsilon \psi_{n,1} \\ \psi_{n,1} e^{i\phi_1} + \psi_{n,3} + r \psi_{n,5} e^{-ik} = \varepsilon \psi_{n,2} \\ \psi_{n,1} + \psi_{n,2} + r \psi_{n,4} = \varepsilon \psi_{n,3} \\ r \psi_{n,3} + \psi_{n,5} + \psi_{n,6} = \varepsilon \psi_{n,4} \\ \psi_{n,4} + r \psi_{n,2} e^{-ik} + \psi_{n,6} e^{i\phi_2} = \varepsilon \psi_{n,5} \\ \psi_{n,4} + r \psi_{n+1,1} + \psi_{n,5} e^{-i\phi_2} = \varepsilon \psi_{n,6} \end{cases} \quad (8)$$

where $\varepsilon = \frac{E}{t_c}$. Rewriting Eq.(8) to a matrix form, we can express it in terms of a transfer matrix form,

$$\begin{pmatrix} \psi_{n+1,1} \\ \psi_{n,6} \end{pmatrix} = M(\varepsilon) \begin{pmatrix} \psi_{n,1} \\ \psi_{n-1,6} \end{pmatrix} \quad (9)$$

where M is a 2×2 matrix and its elements are

$$\begin{aligned} M_{11}(\varepsilon) &= e^{i \frac{k+\phi_1-\phi_2}{2}} \frac{l_4 l_5 - r^2 l_1^2}{r^2 l_1 l_2} \\ M_{12}(\varepsilon) &= -e^{i \frac{k+\phi_1-\phi_2}{2}} \frac{l_5}{r l_1} \\ M_{21}(\varepsilon) &= e^{i \frac{k+\phi_1-\phi_2}{2}} \frac{l_4}{r l_1} \\ M_{22}(\varepsilon) &= -e^{i \frac{k+\phi_1-\phi_2}{2}} \frac{l_2}{l_1} \end{aligned}$$

where

$$\begin{aligned} l_1 &= 2[(\varepsilon^2 - r^2) \cos \frac{k + \phi_1 - \phi_2}{2} + \\ &\quad 2\varepsilon \cos \frac{k}{2} \cos \frac{\phi_1 + \phi_2}{2} + \cos \frac{k - \phi_1 + \phi_2}{2}] \\ l_2 &= 1 + r^4 - 2(1 + r^2)\varepsilon^2 + \varepsilon^4 - 2r^2 \cos k \\ l_3 &= \varepsilon(3 + 2r^2 + r^4 - 2(2 + r^2)\varepsilon^2 + \varepsilon^4) - 2r^2 \varepsilon \cos k \\ l_4 &= l_3 + 2(1 - \varepsilon^2) \cos \phi_1 - 2r^2 \cos(k + \phi_1) \\ l_5 &= l_3 + 2(1 - \varepsilon^2) \cos \phi_2 - 2r^2 \cos(k - \phi_2) \end{aligned}$$

We assume that the width L_1 of the star lattice contains an integer number of the unit cells, we can get the reduced transfer matrix

$$\begin{pmatrix} \psi_{L_1+1,1} \\ \psi_{L_1,6} \end{pmatrix} = (M(\varepsilon))^{L_1} \begin{pmatrix} \psi_{1,1} \\ \psi_{0,6} \end{pmatrix} \quad (10)$$

Considering the boundary condition $\psi_{L_1,6} = \psi_{0,6} = 0$, the edge energy ε_{edge} satisfies $(M(\varepsilon))^{L_1}_{21} = 0$.^{4,5} For $L_1 \gg 1$, the criterion for edge states follows^{4,5}

$$|(M(\mu_j))_{11}| \begin{cases} < 1 & \text{edge states localized in site 1} \\ > 1 & \text{edge states localized in site } L_x - 1 \\ = 1 & \text{coincide with bulk states} \end{cases} \quad (11)$$

The quantum Hall conductance of systems can be expressed in terms of the Chern number of $U(1)$ bundle over the magnetic Brillouin zone.³ The bulk-edge correspondence theory reveals that the Chern number $C(\mu_j)$ is equivalent to the winding number of the edge state moving around the hole of Riemann surface (the complex-energy surface), namely the intersection number between the canonical loop on the Riemann surface and the trace of the edge state energy μ_j .⁴⁻⁶ (see Fig. 3). Thus, the quantum Hall conductance can be given by the winding number of the edge states, $\sigma_{xy}^{edge} = -\frac{e^2}{h} C(\mu_j)$ when the Fermi energy lies in the j th energy gap. Therefore, we can count the Chern number from the energy spectrum of the system.

The mean field studies of the star lattice with the Hamiltonian of Eq.(1) give various spin liquid phases.¹⁹ It is worth studying that the topological properties of these spin liquid phases.

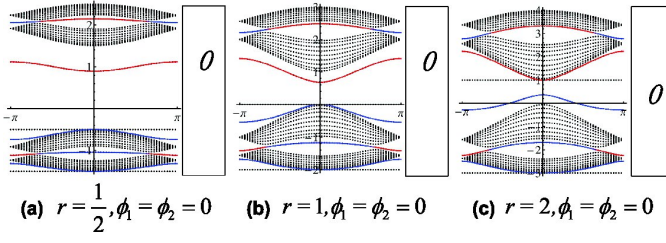


FIG. 4: (Color online) The energy spectra of $SL[0,0,0]$ for $r = 1/2$ in (a), $r = 1$ in (b), and $r = 2$ in (c).

B. Uniform spin liquid phase: $SL[0,0,0]$

The uniform spin liquid phase, $SL[0,0,0]$ respects all the space-group symmetry of the lattice and time reversal symmetry. The energy spectra of the $SL[0,0,0]$ phase for several set of parameters (r, ϕ) are plotted in Fig. 4. It can be seen that both of the bulk energy band and edge states are k-symmetric, $E(k) = E(-k)$, due to the space inverse symmetry, but the edge states are either embedded in the bulk states or isolated in the gap, namely there is no nontrivial bulk gap. Interestingly there exist two flat bands lying in the energy-band gap and touching an edge-state band, which is caused by interference.²⁵ It is similar to a uniform spin liquid on the kagome lattice and can be spoiled by perturbations, such as the next nearest neighbor hopping.¹⁹ Thus, the Chern number is not well-defined and corresponds to common metals or insulators without IQHE. Actually the interactions from spinons can lead to instability of the uniform spin liquid phase to develop to the phases with breaking time reversal symmetry.¹⁹

C. Nematic spin liquid phase: $SL[\phi, -\phi, 0]$

The spin liquid phases are characterized by a set of spin chirality operators.¹⁹ Different chiral spin phases exhibit different local magnetic fluxes. For the nematic spin liquid phase $SL[\phi, -\phi, 0]$, time reversal symmetry is broken spontaneously,¹⁹ we plot the energy spectra for some parameter (r, ϕ) in Fig. 5. It can be seen that the k-symmetries of both bulk bands and edge states are broken, $E(k) \neq E(-k)$. It shows that time reversal symmetry breaking could induce space inverse symmetry breaking that breaks the k-symmetries of bulk bands and edge states. However, the edge states are also either embedded in the bulk states or isolated in the gap. This implies the systems are common metals or insulators, but without IQHE, as $SL[0,0,0]$ phase.

D. Chiral spin liquid phase I: $SL[\phi, \phi, -2\phi]$

For the chiral spin liquid phase I $SL[\phi, \phi, -2\phi]$, time reversal symmetry is also broken spontaneously.¹⁹ In

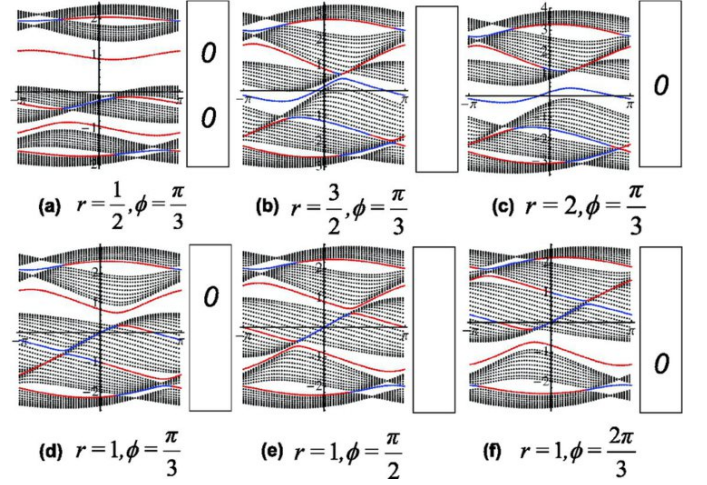


FIG. 5: (Color online) The energy spectra of $SL[-\phi, \phi, 0]$ for different parameters (r, ϕ).

principle, the Chern number in the j th gap between the bulk energy bands depends on the parameters r and ϕ , $C_j(r, \phi)$ (here we use this symbol for Chern number). However, we find from numerical investigations that the Chern number in the range of r and ϕ obeys the following symmetries :

- (1) $C_j(r, 2\pi - \phi) = -C_j(r, \phi)$ for $\phi \in (0, \pi)$;
- (2) $C_j(r, \pi + \phi) = -C_{5-j}(r, \phi)$ for $\phi \in (0, \pi)$;
- (3) $C_j(r, \phi) = C_j(-r, \phi)$ for $\phi \in (0, 2\pi)$;

Thus, we can restrict the parameters only in the range of $\phi \in (0, \frac{\pi}{2})$ and $r > 0$. In Fig. 6 we plot the energy spectrum for some typical parameters (t, ϕ) and $L_1 = 10$. The Chern number can be counted by the winding number of the torus formed by two Riemann surfaces.⁴ (see Fig. 3). The numbers in the right-hand side of each figures in Figs. 6 are the Chern number of the system when the Fermi energy lies in the corresponding energy gap. It can be seen that the bulk energy spectrum is k-symmetric, $E(k) = E(-k)$ even though $\phi \neq 0$, but the edge state has no k-symmetry. It implies that the space inversion symmetry still holds due to the bulk band k-symmetry, but the spontaneous time reversal breaking breaks the edge state k-symmetry. Different Chern number implies different topological orders of the system. In order to give the phase diagram in the parameter space, we try to find out the critical lines in the parameter space. When the energy gaps close, the Chern number must change, namely a phase transition happens. Notice that the bulk spectrum has the Krammers degeneracy, $E(k) = E(-k)$, it implies that the close of the energy gap of the bulk band happens only at the Γ point ($k = 0$). Thus, we solve the eigenenergies of the unit cell Hamiltonian (bulk band) at $k = 0$. Numerical investigation indicates the bulk energy bands at $k = 0$ are linear with r , which allows us suppose that the eigenenergies of the bulk energy band at $k = 0$ have the form $E_i(k = 0) = \pm r + b_i(\phi)$, where $i = 1, 2, 3$. Substituting this form into the eigen equation of the Hamiltonian of the two-dimensional star

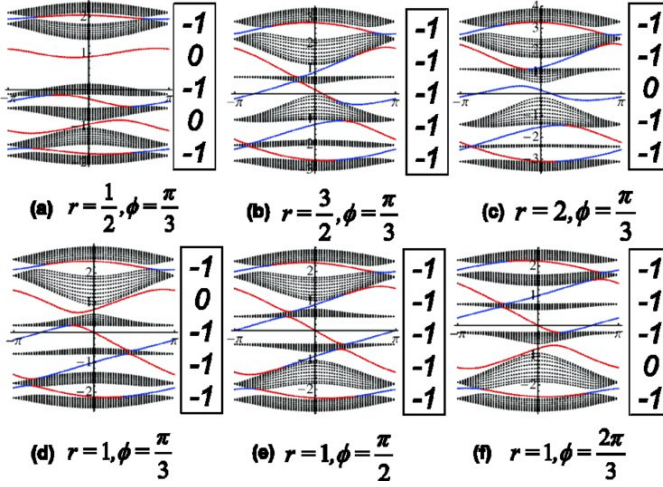


FIG. 6: (Color online) The energy spectra of $SL[\phi, \phi, -2\phi]$ for different parameters (r, ϕ) .

lattice in the k space we can find that $b_i(\phi)$ satisfies a cubic equation,

$$b^3 - 3b - 2\cos\phi = 0 \quad (12)$$

When we consider $\phi \in (0, \frac{\pi}{2})$, the solutions of the above cubic equation are

$$\begin{cases} b_1 = 2\cos\frac{\phi+2\pi}{3} \\ b_2 = -2\cos\frac{\phi+\pi}{3} \\ b_3 = 2\cos\frac{\phi}{3} \end{cases} \quad (13)$$

which we set $b_1 < b_2 < b_3$. The closes of the bulk energy band gaps yield the critical lines in the parameter space,

$$\begin{cases} r_{c,1} = \sqrt{3}\sin\frac{\phi}{3} \\ r_{c,2} = \sqrt{3}\sin\frac{\pi-\phi}{3} \\ r_{c,3} = \sqrt{3}\sin\frac{\phi+\pi}{3} \end{cases} \quad (14)$$

These three functions separate the parameter space $r - \phi$ into several different regions which have different topological orders shown in Fig. 7. Different regions in the phase diagram represent the ground states with different Chern number configurations in which the Chern number in different positions corresponds to the Fermi energy in different gaps like Fig. 5. The phases with different Chern numbers reflect different integer quantum Hall conductance of the system.

E. Chiral spin liquid phase II: $SL[\phi_1, \phi_2, -(\phi_1 + \phi_2)]$

For more general chiral spin liquid phases II $SL[\phi_1, \phi_2, -(\phi_1 + \phi_2)]$, the time reversal and space inverse symmetries are broken spontaneously. For example, the energy spectra of the spin liquid phase $SL[\frac{\phi}{3}, \frac{2\phi}{3}, -\phi]$ for some specific parameters are shown in Fig. 8. It can be seen that the k -symmetries of both bulk bands and edge

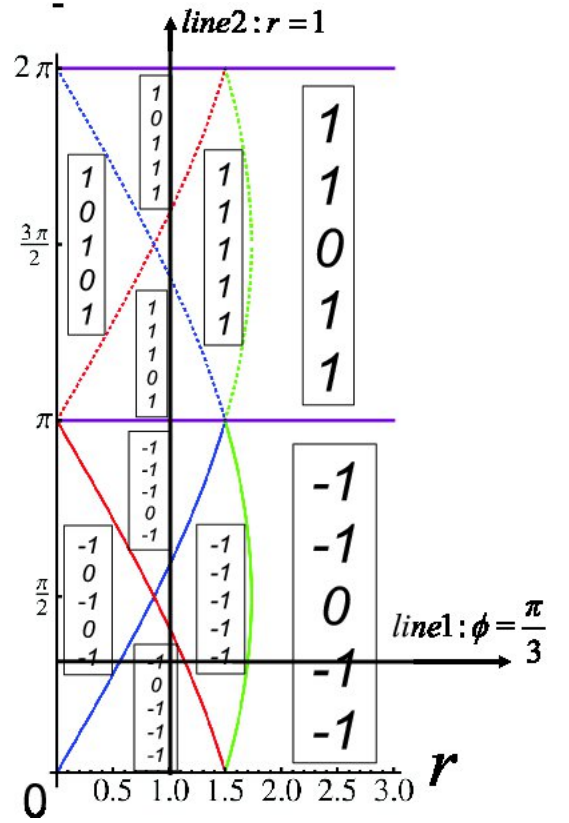


FIG. 7: The phase diagram of $SL[\phi, \phi, -2\phi]$. Different region represents different Chern numbers for various filling fraction, which are even functions of r and periodic functions of ϕ with periodicity 2π . The energy spectrum along line 1 and line 2 are shown along (a) \rightarrow (d) \rightarrow (b) \rightarrow (c) and (d) \rightarrow (e) \rightarrow (f) in Fig. 6 respectively.

state are broken $E(k) \neq E(-k)$, and the Chern numbers in some energy gaps are not well-defined, such as the top three gaps for $r = 1, \phi_1 = \frac{2\pi}{3}$ and $\phi_2 = \frac{4\pi}{3}$. Because the degenerate points of the bulk band and edge state are not at the $k = 0$ point, the phase transition lines can not be solved easily.

TABLE I: The energy band properties of different spin liquid phases

	EKS	BKS	TRS	SIS	Chern number			
					r :	$\frac{1}{2}$	1	2
$SL[0, 0, 0]$	yes	yes	yes	yes		-1	-1	x
$SL[\frac{\pi}{3}, -\frac{\pi}{3}, 0]$	no	no	no	no		x	x	0
$SL[\frac{\pi}{3}, \frac{\pi}{3}, -\frac{2\pi}{3}]$	no	yes	no	yes		-1	-1	0
$SL[\frac{\pi}{3}, \frac{2\pi}{3}, -\pi]$	no	no	no	no		0	-1	0

EKS: Edge-state k -symmetry; BKS: Bulk band k -symmetry; TRS: Time reversal symmetry; SIS: Space inverse symmetry; x: non-well-defined Chern number.

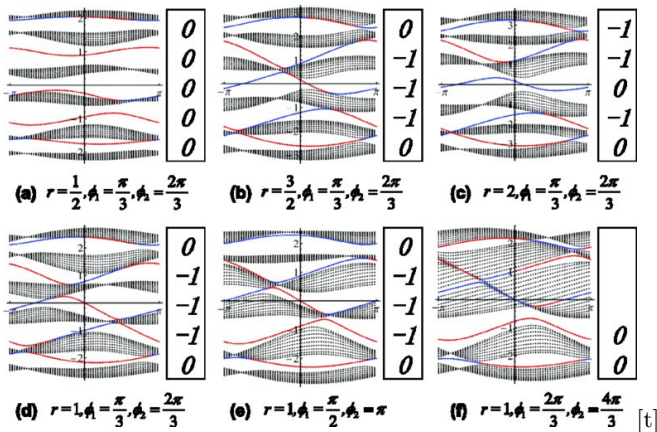


FIG. 8: (Color online) The energy spectra of $SL[\phi_1, \phi_2, -(\phi_1 + \phi_2)]$ for different parameters (r, ϕ).

IV. DISCUSSIONS

To compare the basic energy-band properties of different spin liquid phases, we assume that the Fermi energy lies in the middle of the middle energy-band gap. The energy band symmetry and Chern numbers for some specific cases are listed in Table I.

It can be seen from Table I that for $SL[0, 0, 0]$ both of the edge k-symmetry (EKS) and bulk k-symmetry (BKS) are held due to the time reversal invariance and space inversion invariance. When $r > 2$, the Chern number becomes non-well-defined. The cases in the 2 ~ 4 lines in Table I indicate that there is no EKS, but BKS remains for $SL[\frac{\pi}{3}, \frac{\pi}{3}, -\frac{2\pi}{3}]$. This implies that the spontaneous time reversal symmetry breaking does not always induce the space inversion symmetry breaking and the EKS can be broken by the time reversal symmetry.

The results in Table I reveal that the Chern number depends on not only the time reversal and space inverse symmetries, but also the parameters ($r, \phi_1, \phi_2, \phi_{12}$) of the star lattice. The ground states become normal metals or semiconductors for the phases without the well-defined Chern number. Interestingly, there is a topological invariance for the exchange of the magnetic fluxes in the two triangles $SL[\phi_1, \phi_2, -(\phi_1 + \phi_2)]$ and $SL[\phi_2, \phi_1, -(\phi_1 + \phi_2)]$. They have the same Chern numbers and their bulk energy bands are k-asymmetric. These findings indicate some new phases in the 2-

dimensional materials.²⁶

V. CONCLUSIONS

In summary, we have studied the edge states and their topological orders in the different spin liquid phases of star lattice by using the bulk-edge correspondence theory. The bulk and edge-state energy structures and Chern number depend on the spin liquid phases and hopping parameters because the local spontaneous magnetic flux in the spin liquid phases breaks the time reversal and space inversion symmetries. We have given the characteristics of bulk and edge energy structures and their corresponding Chern numbers in the uniform, nematic and chiral spin liquid phases. In particular, we have obtained analytically the phase transition lines of different topological phases and their corresponding phase diagrams for the chiral spin liquid states $SL[\phi, \phi, -2\phi]$. We have also found that the topological invariance for the spin liquid phases, $SL[\phi_1, \phi_2, -(\phi_1 + \phi_2)]$ and $SL[\phi_2, \phi_1, -(\phi_1 + \phi_2)]$. The results tell us the relationship between the energy-band and edge-state structures and their topological orders of the star lattice. Especially, this star lattice has been synthesized in the material called iron acetate recently.²⁷ Therefore, our results provide a Hall conductance experimental guideline to discriminate the spin liquid phases in real materials and cold atoms in optical lattice. The changes of filling fraction could be implemented by tuning the applied gate voltage. These results can also give some hints for understanding the Heisenberg model on the star lattice.

Acknowledgments

We thank Ming-Liang Tong and Xiao-Ming Chen for helpful discussions. G.-Y. Huang thanks An Zhao and Jie-Sen Li for useful discussions on numerical calculations. This work is supported by the Fundamental Research Funds for the Central Universities of China (11lgjc12 and 10lgzd09), NSFC-11074310, MOST of China 973 program (2012CB821400), Specialized Research Fund for the Doctoral Program of Higher Education (20110171110026), and NCET-11-0547.

* Electronic address: stslsd@mail.sysu.edu.cn

† Electronic address: yaodaaox@mail.sysu.edu.cn

¹ R. B. Laughlin, Phys. Rev. B 23, 5632(1981)

² B. I. Halperin, Phys. Rev. B 25, 2185 (1982)

³ D. J. Thouless, M. Kohmoto, M. P. Nightingale and M. den Nijs, Phys. Rev. Lett. 49, 405 (1982)

⁴ Y. Hatsugai, Phys. Rev. Lett. 71, 3697 (1993).

⁵ Y. Hatsugai, Phys. Rev. B 48, 11851 (1993).

⁶ Zhigang Wang, Ping Zhang, New J. Phys. 11, 123014 (2010)

⁷ Y. Shimizu, K. Miyagawa, K. Kanoda, M. Maesato and G. Saito, Phys. Rev. Lett. 91, 107001 (2003)

⁸ Matthew P. Shores, Emily A. Nytko, Bart M. Bartlett and Daniel G. Nocera, J. Am. Chem. Soc. 127, 13462(2005)

⁹ M. Sasaki, K. Hukushima, H. Yoshino and H. Takayama, Phys. Rev. Lett. 99, 137202 (2007)

- ¹⁰ Yi Zhou, Patrick A. Lee, Tai-Kai Ng and Fu-Chun Zhang, Phys. Rev. Lett. 101, 197201 (2008)
- ¹¹ Michael J. Lawler, Arun Paramakanti, Yong Baek Kim and Leon Balents, Phys. Rev. Lett. 101, 197202 (2008)
- ¹² P. Nikolic and T. Senthil, Phys. Rev. B 68, 214415 (2003)
- ¹³ Rajiv R. P. Singh and David A. Huse, Phys. Rev. B 76, 180407(R) (2007)
- ¹⁴ J. B. Marston and C. Zeng, J. Appl. Phys. 69, 5962 (1991)
- ¹⁵ A. Kitaev, Ann. Phys. (N.Y.) 321, 2 (2006).
- ¹⁶ H. Yao and S. A. Kivelson, Phys. Rev. Lett. 99, 247203 (2007).
- ¹⁷ G. Kells, D. Mehta, J. K. Slingerland, and J. Vala, Phys. Rev. B 81, 104429 (2010).
- ¹⁸ K. Ohgushi, S. Murakami, and N. Nagaosa, Phys. Rev. B 62, R6065 (2000)
- ¹⁹ B.-J. Yang, A. Paramakanti, Y.B. Kim, Phys. Rev. B 81, 134418(2010).
- ²⁰ T. P. Choy and Y. B. Kim, Phys. Rev. B 80, 064404 (2009).
- ²¹ A. Rüegg, J. Wen, and G. A. Fiete, Phys. Rev. B 81, 205115 (2010).
- ²² Jun Wen, Andreas Rüegg, Joseph C.-C. Wang and Gregory A. Fiete Phys. Rev. B 82, 075125 (2010)
- ²³ Y. Hatsugai, T. Fukui, and H. Aoki, Phys. Rev. B 74, 205414 (2006)
- ²⁴ Zhigang Wang and Ping Zhang Phys. Rev. B 77, 125119 (2008)
- ²⁵ H. Aoki, M. Ando, and H. Matsumura, Phys. Rev. B 54, R17296 (1996).
- ²⁶ Nagaosa, Science 318, 758(2007).
- ²⁷ Y.-Z. Zheng, M.-L. Tong, W. Xue, W.-X. Zhang, X.-M. Chen, F. Grandjean, and G. J. Long, Angew. Chem., Int. Ed. 46, 6076(2007)